(0.003 mol) was dissolved in 15 ml of ethanol and a solution of AgNO$_3$ (slightly in excess of 0.003 mol) dissolved in 25 ml of hot ethanol was added. The precipitate of AgCl was separated by filtration after warming the solution for a few minutes. From the filtrate ethanol was removed. The residue was dissolved in a minimum quantity of chloroform and benzene (15 ml) was added. On standing, black crystals of (NO$_3$)(salNMe$_2$)Cu separated in 80% yield.

(h) **Reaction of (Cl)(salNEt$_2$)Cu with AgClO$_4$.** Dry AgClO$_4$ (0.005 mol) was dissolved in 15 ml of 95% ethanol and this solution was added to a solution of (Cl)(salNEt$_2$)Cu (0.005 mol) in 15 ml of ethanol. The precipitated AgCl was filtered. The volume of the filtrate was reduced to 10 ml followed by the addition of water (30 ml) and the solution was stirred magnetically at room temperature. Blue crystals of the composition [(H$_2$O)(salNEt$_2$)Cu] ClO$_4$·2H$_2$O started separating within 2 hr. The trihydrate when dried at 100° for 5 hr at 5 mm gave brown [(H$_2$O)(salNEt$_2$)Cu] ClO$_4$.

Physical Measurements. Magnetic moments were studied using a Gouy balance described elsewhere.[16] Electronic spectra were studied on a Cary Model 14 spectrometer. Solids were examined in finely dispersed hydrocarbon mulls sandwiched between quartz plates.

(16) T. S. Kannan and A. Chakravorty, *Inorg. Chem.*, **9**, 1153 (1970).

Infrared spectra were recorded on a Perkin-Elmer 521 recording spectrometer. Conductivity measurements were made in nitromethane at 18° using a Systronics (India) bridge. Molecular weights were determined cryoscopically in thiophene-free dry benzene.

Magnetic Exchange in Oxalate- and Squarate-Bridged Nickel(II) Dimer Complexes

D. MICHAEL DUGGAN,[1] E. KENT BAREFIELD, and DAVID N. HENDRICKSON*

Variable-temperature (4.2–290°K) magnetic susceptibilities were determined for one squarate-bridged and two oxalate-bridged nickel(II) dimers. Antiferromagnetic interactions were detected in both types of dimers; the oxalate-bridged dimers have $J \simeq -17$ cm^{-1}, whereas the squarate-bridged dimer has $J \simeq -0.4$ cm^{-1}. The magnetic exchange mechanism is discussed and symmetry considerations are delineated.

Introduction

Nickel(II) cluster compounds have been the focal points of several recent magnetic susceptibility studies.[2] Complexes have been found with antiferromagnetic exchange interactions as well as ferromagnetic interactions. In fact, linear trimeric bis(acetylacetonato)nickel(II) has been reported[3] to have both ferromagnetic coupling ($J = +26$ cm^{-1}) between adjacent nickel atoms and antiferromagnetic coupling ($J = -7$ cm^{-1}) between the terminal nickel atoms. Linear-chain one-dimensional antiferromagnetism has been detected for CsNiCl$_3$.[4] Very recently Ginsberg[2,5] reported the first example, in a cluster complex, of ferromagnetic exchange coupling between metal atoms linked by polynuclear bridges (thiocyanate groups) in [Ni$_2$(en)$_4$(NCS)$_2$]I$_2$.

Oxalate-bridged metal dimers have been known for some time.[6] Crystal structures have been reported for FeC$_2$O$_4$·2H$_2$O,[7] Cu(NH$_3$)$_2$C$_2$O$_4$,[8] (NH$_4$)$_2$[UO$_2$(C$_2$O$_4$)$_3$],[9]

Ti$_2$(C$_2$O$_4$)$_3$·10H$_2$O,[10] and [Ru$_2$(py)$_8$(C$_2$O$_4$)](BF$_4$)$_2$.[11] The oxalate bridge is planar and bis bidentate. Curtis has reported[12,13] the preparation of various oxalate-bridged nickel dimers. In the following we report the results of a magnetic susceptibility study of some nickel dimers bridged either by oxalate or by squarate (C$_4$O$_4^{2-}$). We address ourselves to two main questions: "How will the magnetic interaction between the nickel(II) atoms compare between oxalate- and squarate-bridged dimers and what type of magnetic interaction will the oxalate triatomic bridge propagate, given the observation that the thiocyanate bridge leads to a net ferromagnetic interaction?" The latter question is relevant in that the thiocyanate-bridged nickel dimer is the only other triatomic-bridged nickel(II) complex studied magnetically.

Theory

The ground state of Ni(II) in an octahedral environment is orbitally nondegenerate and as such we represent intradimer magnetic interactions with the isotropic spin Hamiltonian

$$\hat{H} = -2J\hat{s}_1 \cdot \hat{s}_2 \tag{1}$$

Here J is the exchange integral and $\hat{s}_1$ is a spin operator. The

(1) Esso Fellow, 1971–1972.

(2) A. P. Ginsberg, *Inorg. Chim. Acta Rev.*, **5**, 45 (1971).

(3) A. P. Ginsberg, R. L. Martin, and R. C. Sherwood, *Inorg. Chem.*, **7**, 932 (1968).

(4) J. Smith, B. C. Gerstein, S. H. Liu, and G. Stucky, *J. Chem. Phys.*, **53**, 418 (1970).

(5) (a) A. P. Ginsberg, R. C. Sherwood, R. W. Brookes, and R. L. Martin, *J. Amer. Chem. Soc.*, **93**, 5927 (1971); (b) A. P. Ginsberg, R. L. Martin, R. W. Brookes, and R. C. Sherwood, *Inorg. Chem.*, **11**, 2884 (1972).

(6) J. Chatt, F. G. Mann, and A. F. Wells, *J. Chem. Soc.*, 2087 (1938).

(7) F. Mazzi and C. Garavelli, *Period. Mineral.*, **26**, 269 (1957).

(8) J. Garaj, *Chem. Commun.*, 904 (1968).

(9) N. W. Alcock, *Chem. Commun.*, 1327 (1968).

(10) M. G. B. Drew, G. W. A. Fowles, and D. T. Lewis, *Chem. Commun.*, 876 (1969).

(11) P. T. Cheng, B. R. Loescher, and S. C. Nyburg, *Inorg. Chem.*, **10**, 1275 (1971).

(12) N. F. Curtis, *J. Chem. Soc.*, 4109 (1963).

(13) N. F. Curtis, *J. Chem. Soc. A*, 1584 (1968).

molar paramagnetic susceptibility for a Ni(II) dimer ($s_1 = s_2 = 1$) can be shown to be[14]

$$\chi_M = \frac{Ng^2\beta^2}{3k(T-\Theta)}\left\{\frac{30\exp(6J/kT)+6\exp(2T/kT)}{5\exp(6J/kT)+3\exp(2J/kT)+1}\right\}+N\alpha \quad (2)$$

In this expression N, β, k, and T have their usual meaning and it is assumed that $g_x = g_y \cong g_z \equiv g$. The Curie–Weiss constant Θ has the effect of correcting for intercluster interaction. The last term ($N\alpha$) in eq 2 is the temperature-independent paramagnetism (TIP).

Ginsberg, *et al.*,[5b] have considered the effects of single-ion zero-field interactions on the magnetic susceptibility of nickel dimers. In their treatment they have treated intercluster interaction with the molecular field approximation where the Hamiltonian for this interaction is taken as $-2Z' \cdot J'\hat{S}_z\langle\hat{S}_z\rangle$. Here $\hat{S}_z$ is the operator for the z component of total dimer spin, J' is the effective interdimer exchange integral, and Z' is the dimer lattice coordination number. The molar paramagnetic susceptibility for a nickel(II) dimer was shown to be

$$\chi_M = \frac{2Ng^2\beta^2}{3k}\left\{\frac{F_1}{T-4Z'J'F_1}+\frac{2F'}{1-4Z'J'F'}\right\}+N\alpha \quad (3)$$

where

$$F' = F_2/D + 3C_2{}^2F_3/(3J-\delta) + 3C_1{}^2F_4/(3J+\delta) \quad (4)$$

$$F_1 = \frac{1+e^{4J/kT}+4e^{4J/kT}e^{D/kT}}{2+e^{D/kT}+e^{J/kT}e^{-\delta/kT}+e^{J/kT}e^{\delta/kT}+2e^{4J/kT}+2e^{4J/kT}e^{D/kT}} \quad (5)$$

$$F_2 = \frac{2e^{4J/kT}e^{D/kT}+e^{D/kT}-1-2e^{4J/kT}}{2+e^{D/kT}+e^{J/kT}e^{-\delta/kT}+e^{J/kT}e^{\delta/kT}+2e^{4J/kT}+2e^{4J/kT}e^{D/kT}} \quad (6)$$

$$F_3 = \frac{e^{4J/kT}-e^{J/kT}e^{\delta/kT}}{2+e^{D/kT}+e^{J/kT}e^{-\delta/kT}+e^{J/kT}e^{\delta/kT}+2e^{4J/kT}+2e^{4J/kT}e^{D/kT}} \quad (7)$$

$$F_4 = \frac{e^{4J/kT}-e^{J/kT}e^{-\delta/kT}}{2+e^{D/kT}+e^{J/kT}e^{-\delta/kT}+e^{J/kT}e^{\delta/kT}+2e^{4J/kT}+2e^{4J/kT}e^{D/kT}} \quad (8)$$

$$\delta = [(3J+D)^2-8JD]^{1/2} \quad (9)$$

$$C_1 = 2(2)^{1/2}D/[(9J-D+3\delta)^2+8D^2]^{1/2} \quad (10)$$

$$C_2 = (9J-D+3\delta)/[(9J-D+3\delta)^2+8D^2]^{1/2} \quad (11)$$

In these expressions D is the single-ion zero-field splitting parameter. As with eq 2, eq 3 was derived by assuming $g_x = g_z = g$.

Equations 2 and 3 will be used to fit the magnetic susceptibility data for the squarate- and oxalate-bridged nickel(II) dimers. Ginsberg[5b] has shown that the evaluation of accurate g and J parameters for a given nickel dimer will not be influenced markedly by the value of either the zero-field splitting parameter D or the intercluster interaction $Z'J'$. We have also investigated this by taking a set of parameters (J, g, $N\alpha$) close to those we found for the oxalate-bridged nickel dimers (see Results and Discussion) and varying D and $Z'J'$. In Figure 1 we see that the effect of a
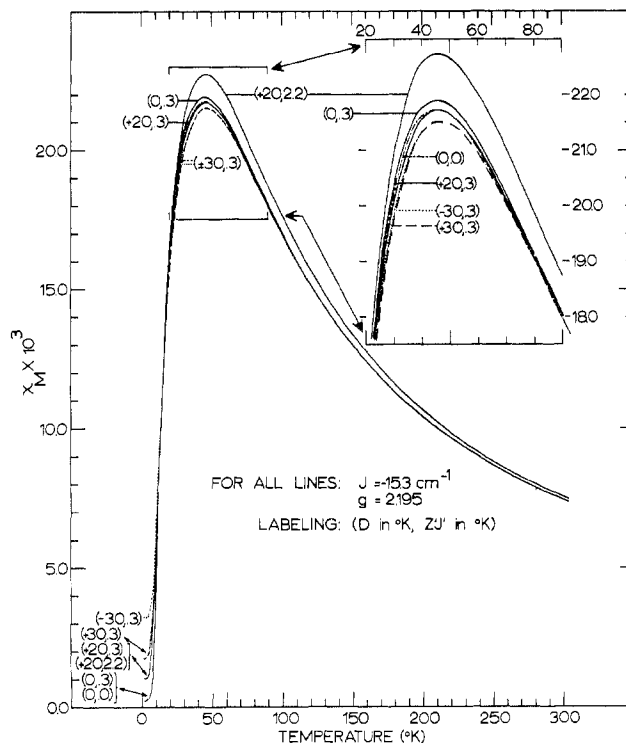

Figure 1. Molar paramagnetic susceptibility *vs.* temperature curves indicating the effects of variations of $\pm D$ and $Z'J'$ on a typical antiferromagnetic curve.

large variance in D and $Z'J'$ is only to displace the χ *vs.* temperature curve along the χ axis. The position of the maximum is essentially unchanged and since this position determines the value of J, the value of D or $Z'J'$ has little effect on the evaluation of J.

Experimental Section

Compound Preparation. All reactants, unless otherwise specified, were reagent grade. Analytical work was carried out by the microanalytical laboratory of the School of Chemical Sciences, University of Illinois.

Triethylenetetramine (trien) was purchased from Aldrich and used as received. Samples of dihydroxycyclobutenedione (squaric acid) were made as reported[15] and also purchased from Aldrich. The nickel complex of the macrocyclic ligand *meso*-2,4,4,9,9,11-hexamethyl-1,5,8,12-tetraazacyclotetradecane was prepared by a reported recipe.[16] Preparation of the nickel(II) oxalate- and squarate-bridged dimers was effected by mixing an aqueous solution of $Ni(ClO_4)_2\cdot 6H_2O$ and tetramine or Ni(macrocycle)$^{2+}$ with an aqueous solution of either sodium oxalate or sodium squarate. Solid samples were dried *in vacuo* over P_2O_5. Analytical data can be found in Table I.

Physical Measurements. Variable-temperature (4.2–290°K) magnetic susceptibilities were measured with a Princeton Applied Research Model 150A vibrating sample magnetometer. The superconducting magnet was operated at two field strengths, 14.8 and 54.3 kG. A calibrated gallium arsenide diode is used in the temperature-controlling and -sensing device. In these measurements $CuSO_4\cdot 5H_2O$ was used as a standard. Corrections for the diamagnetism of the sample container and background were applied at all temperatures. Pascal constants were used to correct for the diamagnetism of the compounds. The absolute accuracy of molar susceptibilities measured on this apparatus is believed to be $\pm 2\%$.

The least-squares fitting of the magnetic susceptibility curves was carried out using STEPT, a computer function minimization program written by J. P. Chandler (Indiana University). The simplex method[17] is used in the minimization. The function minimized is given as

(14) A. Earnshaw, B. N. Figgis, and J. Lewis, *J. Chem. Soc. A*, 1656 (1966).

(15) G. Maahs, *Justus Liebigs Ann. Chem.*, **686**, 55 (1965).

(16) N. F. Curtis, *Coord. Chem. Rev.*, 3, 1 (1968).

(17) J. A. Nelder and R. Mead, *Comput. J.*, 308 (1965).

Table I. Analytical Data

	%C		%H		%N		%Ni	
Compd	Calcd	Found	Calcd	Found	Calcd	Found	Calcd	Found
$[Ni_2(trien)_2(C_2O_4)](ClO_4)_2$	24.13	24.19	5.21	4.96	16.08	15.80	16.85	16.77
$[Ni_2(macro)_2(C_2O_4)](ClO_4)_2$	41.96	42.02	7.46	7.52	11.51	11.35	12.06	11.93
$[Ni_2(macro)_2(C_4O_4)](ClO_4)_2$	43.36	43.36	7.28	7.21	11.24	11.22	11.77	11.77

$$\Delta = \sum_i^{NP} \left\{ [\chi_M(obsd)_i - \chi_M(calcd)_i] T^N \right\}^2$$

where NP is the number of experimental points and N can be adjusted to emphasize selectively the regions of the susceptibility curve which should be fit the closest. Generally, fits to eq 3 were effected by using $N = 0$.

The goodness of fit, or standard error of estimate SE, was gauged by using the expression suggested by Ginsberg[5b]

$$SE = \left\{ \sum_{i=1}^{NP} [\mu_{eff}(obsd)_i - \mu_{eff}(calcd)_i]^2/(NP - k) \right\}^{1/2}$$

In this expression k is the number of parameters used to fit the NP data points.

Results and Discussion

Variable-temperature (4.2–290°K) magnetic susceptibility data are given in Tables II and III for three compounds: $[Ni_2(trien)_2(C_2O_4)](ClO_4)_2$, $[Ni_2(macro)_2(C_2O_4)](ClO_4)_2$, and $[Ni_2(macro)_2(C_4O_4)](ClO_4)_2$. The tetradentate ligand trien is triethylenetetramine and macro is 2,4,4,9,9,11-hexamethyl-1,5,8,12-tetraazacyclotetradecane, which when
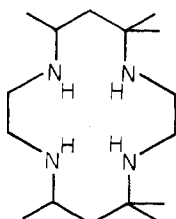
used in its meso form in the presence of base folds to accommodate a chelating ligand. In the above three Ni(II) dimers, oxalate $(C_2O_4{}^{2-})$ and squarate $(C_4O_4{}^{2-})$ have been incorporated as bridging tetradentate ligands. Curtis has shown,[12,13] on the basis of ir data, that the oxalate dianion bridges two nickel moieties in the manner
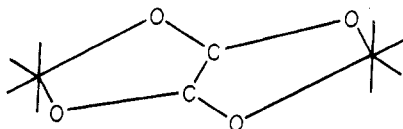
The ir spectra of our nickel(II) oxalate systems indicate that they possess tetradentate oxalate bridges of the sort described by Curtis. X-Ray crystallographic studies on various oxalate complexes of iron,[7] copper,[8] uranyl,[9] titanium,[10] and ruthenium[11] have confirmed this mode of bridging and have shown that the oxalate bridge is planar in each case.

The two oxalate-bridged nickel(II) dimers possess magnetic susceptibility curves indicating antiferromagnetic coupling (Tables II and III). In Figure 2 the χ_M and μ_{eff}/Ni vs. temperature curves are depicted for $[Ni_2(trien)_2(C_2O_4)](ClO_4)_2$ in a magnetic field of 14.8 kG. The susceptibility curve for this compound increases with decreasing temperature until a maximum in χ is reached at 46.5°K. At temperatures below 46.5°K the susceptibility χ_M (and thus μ_{eff}) decreases markedly with decreasing temperature. The μ_{eff}/Ni at
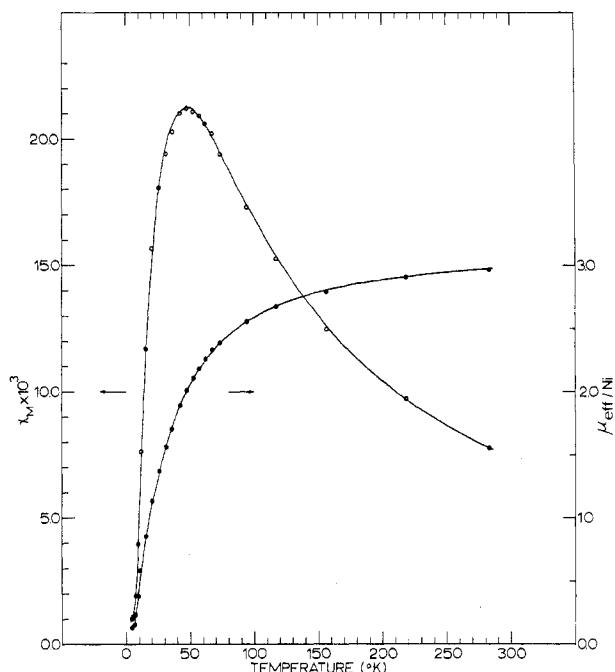
Figure 2. The paramagnetic susceptibility (χ in cgsu/mol) and effective moment (BM per nickel) vs. temperature curves for $[Ni_2(trien)_2(C_2O_4)](ClO_4)_2$ in a magnetic field of 14.8 kG. The circles are the experimental points, whereas the solid lines are theoretical lines, least-squares fit to eq 3 with $J = -15.7$ cm^{-1}, $g = 2.198$, $D = 13.7$ cm^{-1}, and $Z'J' = 0.28°$.

283°K is 2.96 BM, which is in the range expected for an octahedral Ni(II) atom. A comparison of the data for the two oxalate-bridged dimers shows them to have essentially the same magnetic curves. The χ_M vs. temperature curve (see Figure 3) for $[Ni_2(macro)_2(C_2O_4)](ClO_4)_2$ peaks at 48.5°K. It should be pointed out that the susceptibility data for this compound were obtained at a magnetic field strength of 54.3 kG. However, it is clear from Table II that very similar magnetic susceptibility curves are obtained for the trien complex run either at 14.8 kG or at 54.3 kG. Even before we enlist a model to fit our magnetic susceptibility data for the two oxalate-bridged dimers, we know from a comparison of curves that we will get approximately the same parameters for both compounds.

In order to verify that the magnetic interactions which we have described above are indeed due to intramolecular effects and not associated with intermolecular exchange, we have measured the magnetic susceptibility of $[Ni_2(trien)_2C_2O_4]$-$(B(C_6H_5)_4)_2$ from room temperature to liquid helium temperature. Its magnetic properties are essentially the same as for the other oxalate-bridged preparations which have a perchlorate counteranion. This proves that we are dealing with intra- and not intermolecular interactions.

The squarate dianion, like the oxalate dianion, is planar.[18] Our analytical data, as well as a comparison of ir data, show that the squarate also bridges two nickel(II) moieties. The

(18) W. M. Macintyre and M. S. Werhema, *J. Chem. Phys.*, 40, 3563 (1964).

Table II. Experimental and Calculated Magnetic Susceptibility Data for Oxalate-Bridged $[Ni_2(trien)_2(C_2O_4)](ClO_4)_2$[a]

	Low-field data						High-field data				
	Eq 2 $J = -17.3$ cm^{-1} $g = 2.191$ $\Theta = 4.7°$ SE[b] = 0.0272	Eq 3 $J = -15.7$ cm^{-1} $g = 2.198$ $D = 13.7$ cm^{-1} $Z'J' = 0.28°$ SE = 0.0092					Eq 2 $J = -17.6$ cm^{-1} $g = 2.196$ $\Theta = 5.6°$ SE = 0.0487	Eq 3 $J = -16.1$ cm^{-1} $g = 2.179$ $D = 15.6$ cm^{-1} $Z'J' = 2.2°$ SE = 0.0226			
	$10^3 \chi_M$, cgsu			μ_{eff}/Ni, BM			$10^3 \chi_M$, cgsu			μ_{eff}/Ni, BM	
		Calcd			Calcd			Calcd			Calcd
T, °K	Obsd	Eq 2	Eq 3	Obsd	Eq 3	T, °K	Obsd	Eq 2	Eq 3	Obsd	Eq 3
283.0	7.77	7.78	7.82	2.965	2.975	238.0	9.06	9.06	9.03	2.937	2.932
218.3	9.71	9.67	9.71	2.912	2.912	160.5	12.32	12.36	12.39	2.812	2.820
156.7	12.48	12.51	12.57	2.797	2.807	99.5	16.65	16.92	17.07	2.574	2.606
117.2	15.26	15.26	15.36	2.674	2.683	71.6	19.94	19.66	19.86	2.389	2.384
94.5	17.29	17.28	17.41	2.556	2.565	65.0	20.53	20.27	20.46	2.310	2.306
73.6	19.40	19.33	19.49	2.389	2.395	62.5	20.81	20.49	20.66	2.281	2.272
67.5	20.20	19.90	20.06	2.335	2.327	59.4	21.02	20.73	20.88	2.234	2.227
62.0	20.60	20.38	20.53	2.260	2.256	56.6	21.19	20.44	21.05	2.190	2.183
57.1	20.91	20.74	20.88	2.185	2.183	54.0	21.33	21.10	21.18	2.146	2.139
52.7	21.09	21.00	21.10	2.108	2.109	51.3	21.44	21.24	21.27	2.197	2.189
47.8	21.22	21.18	21.23	2.014	2.014	48.2	21.50	21.36	21.31	2.036	2.027
42.6	21.01	21.21	21.14	1.892	1.898	45.0	21.44	21.43	21.27	1.964	1.956
35.8	20.29	20.88	20.56	1.704	1.716	42.5	21.31	21.43	21.16	1.903	1.896
31.5	19.43	20.36	19.81	1.564	1.580	36.3	20.66	21.20	20.56	1.732	1.727
26.0	18.07	19.12	18.22	1.371	1.376	22.5	16.38	18.23	16.28	1.214	1.210
20.5	15.68	16.64	15.49	1.134	1.127	14.0	7.50	10.97	9.20	0.648	0.718
15.7	11.70	12.48	11.53	0.857	0.851	4.2	1.24	0.18	1.09	0.144	0.136
11.7	7.33	7.19	6.84	0.585	0.566						
9.3	3.97	3.85	3.93	0.384	0.382						
7.3	1.94	1.71	2.07	0.238	0.246						
5.6	1.12	0.77	1.22	0.156	0.165						
4.2	1.07	0.15	0.99	0.134	0.129						

[a] Diamagnetic correction from tables (=-331.6×10^{-6}) and TIP assumed to be 200×10^{-6}. [b] Standard error given by the following equation (from ref 5): SE = $\{\Sigma_{i=1}^{n} [\mu_{eff}(obsd)_i - \mu_{eff}(calcd)_i]^2/(n-k)\}^{1/2}$, where n = number of observables and k = number of parameters.

Table III. Experimental and Calculated Magnetic Susceptibility Data for Oxalate-Bridged $[Ni_2(macro)_2(C_2O_4)](ClO_4)_2$ and Squarate-Bridged $[Ni_2(macro)_2(C_4O_4)](ClO_4)_2$[a]

	Oxalate data[b]						Squarate data[c]				
	Eq 2 $J = -18.4$ cm^{-1} $g = 2.194$ $\Theta = 4.2°$ SE[d] = 0.0805	Eq 3 $J = -15.6$ cm^{-1} $g = 2.187$ $D = 20.1$ cm^{-1} $Z'J' = 0.20°$ SE = 0.0516					Eq 2 $J = -1.3$ cm^{-1} $g = 2.210$ $\Theta = 1.6°$ SE = 0.0177	Eq 3 $J = -0.42$ cm^{-1} $g = 2.197$ $D = 15.5$ cm^{-1} $Z'J' = 0.48°$ SE = 0.0192			
	$10^3 \chi_M$, cgsu			μ_{eff}/Ni, BM			$10^3 \chi_M$, cgsu			μ_{eff}/Ni, BM	
		Calcd			Calcd			Calcd			Calcd
T, °K	Obsd	Eq 2	Eq 3	Obsd	Eq 3	T, °K	Obsd	Eq 2	Eq 3	Obsd	Eq 3
237.9	9.07	9.00	8.95	2.938	2.918	183.0	8.73	8.81	8.74	3.143	3.145
160.5	12.19	12.25	12.21	2.797	2.799	218.3	11.16	11.35	11.27	3.121	3.137
99.4	16.42	16.67	16.71	2.555	2.577	156.7	15.80	15.70	15.63	3.147	3.130
71.6	19.23	19.23	19.36	2.346	2.355	117.2	21.09	20.88	20.84	3.144	3.125
65.0	19.74	19.79	19.93	2.265	2.276	73.6	33.45	32.96	33.04	3.138	3.118
62.5	20.08	19.99	20.13	2.240	2.243	47.8	50.58	50.25	50.60	3.109	3.110
59.3	20.34	20.21	20.35	2.196	2.197	31.5	74.06	75.20	76.03	3.054	3.095
56.7	20.33	20.38	20.51	2.147	2.156	17.7	131.2	129.5	130.8	3.047	3.043
54.0	20.64	20.53	20.64	2.111	2.111	11.7	185.7	187.7	188.1	2.948	2.966
51.3	20.75	20.65	20.72	2.063	2.062	9.3	227.4	228.0	227.2	2.908	2.907
48.1	20.83	20.74	20.77	2.002	1.999	7.3	275.9	276.4	274.7	2.838	2.832
45.0	20.84	20.79	20.73	1.937	1.931	6.4	303.5	305.1	303.6	2.787	2.787
42.4	20.76	20.77	20.63	1.876	1.870	5.6	335.2	335.9	335.2	2.740	2.740
36.0	20.38	20.49	20.01	1.713	1.697	5.0	370.0	363.5	364.0	2.720	2.698
22.5	17.19	17.54	16.04	1.244	1.201	4.2	406.8	409.6	411.6	2.614	2.629
14.0	10.83	10.41	9.87	0.779	0.743						
4.2	7.56	0.19	1.99	0.356	0.183						

[a] Diamagnetic corrections used: -562.1×10^{-6} for oxalate; -574.1×10^{-6} for squarate. [b] Data taken at high field = 54.3 kG. [c] Data taken at low field = 14.8 kG. [d] Standard error given by the following equation (from ref 5): SE = $\{\Sigma_{i=1}^{n} [\mu_{eff}(obsd)_i - \mu_{eff}(calcd)_i]^2/(n-k)\}^{1/2}$, where n = number of observables and k = number of parameters.

χ_M and μ_{eff}/Ni *vs.* temperature curves for $[Ni_2(macro)_2(C_4O_4)](ClO_4)_2$ are reproduced in Figure 4. In this case the

χ_M curve does not exhibit a maximum; however, the μ_{eff} curve does show an attenuation of the magnetism for the
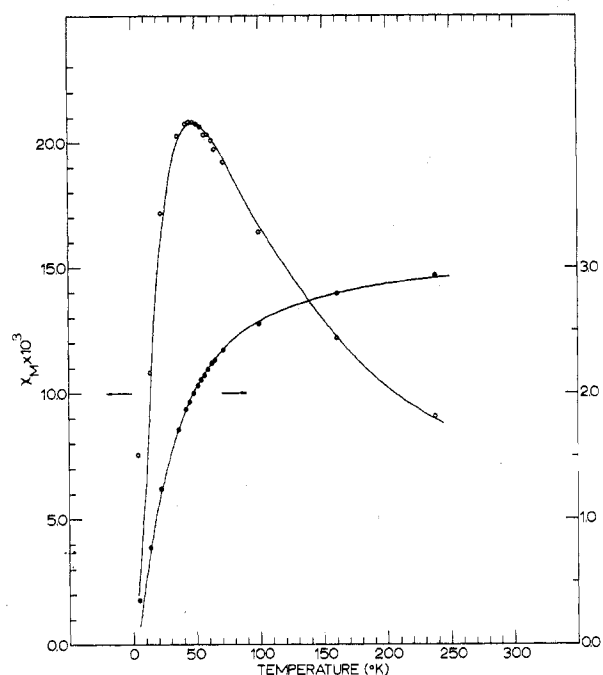
Figure 3. The paramagnetic susceptibility (χ in cgsu/mol) and effective moment (BM per nickel) *vs.* temperature curves for $[Ni_2(macro)_2(C_2O_4)](ClO_4)_2$ in a magnetic field of 54.3 kG. The circles are the experimental points, whereas the solid lines are theoretical lines, least-squares fit to eq 3 with $J = -15.6$ cm^{-1}, $g = 2.187$, $D = 20.1$ cm^{-1}, and $Z'J' = 0.20°$.

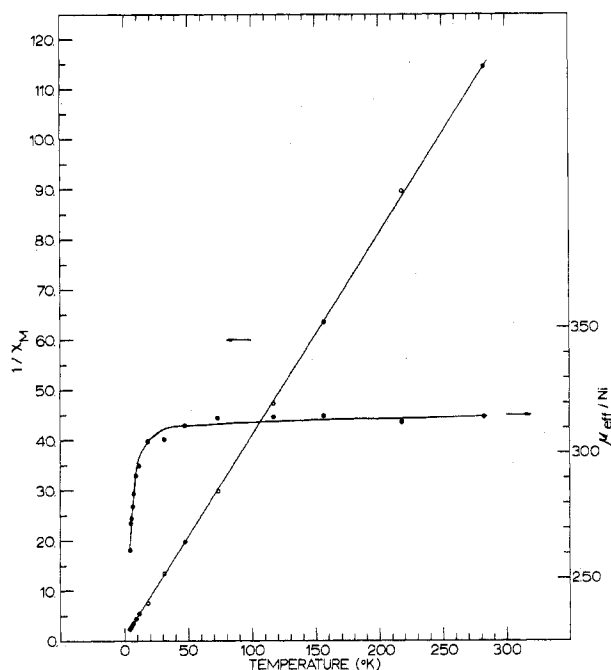**Figure 4.** χ^{-1} and effective moment per nickel *vs.* temperature curves for $[Ni_2(macro)_2(C_4O_4)](ClO_4)_2$ in a magnetic field of 14.8 kG. The circles are the experimental data, whereas the solid lines are a theoretical fit to eq 3 with $J = -0.42$ cm^{-1}, $g = 2.197$, $D = 15.5$ cm^{-1}, and $Z'J' = 0.48°$.

complex at low temperatures. The μ_{eff}/Ni for the squarate-bridged dimer is 3.14 BM at 283°K, remaining relatively unchanged down to 30°K and then falling rapidly to 2.61 BM at 4.2°K. This low-temperature attenuation could be due, in part, to single-ion zero-field interactions. It is clear that the intradimer antiferromagnetic interaction between

two nickel(II) atoms is greatest when they are bridged by the oxalate dianion as opposed to the squarate dianion. This is perhaps as one would expect. In a later section we will entertain a semiquantitative explanation of why this is so, but for now we turn to the results of computer fitting of the χ_M *vs.* temperature curves.

In the Theory we set out two models to explain the magnetism of a given nickel(II) dimer complex. In both models the magnetic exchange is treated as an isotropic exchange, $H = -2Js_1 \cdot s_2$, and an average g is used (*i.e.*, $g_x = g_y \simeq g_z$). The simplest model considered this exchange interaction, temperature-independent paramagnetism ($N\alpha$), and accounted for intercluster interactions with a Curie-Weiss constant Θ, thus giving four parameters: J, g, Θ, and $N\alpha$. In the second model the single-ion zero-field splitting of the Ni(II) atom is also considered and the intercluster interactions are treated by the molecular-field approximation as per Ginsberg.[5b] In this case the parameters are J, g, N, D, and $Z'J'$, where Z' is the average number of nearest clusters and J' is the intercluster interaction parameter.

Least-squares fits to theoretical χ_M expressions were generated for the magnetic susceptibility data and in all cases we assumed that the TIP for the Ni(II) cluster was 200×10^{-6} cgsu. Each set of data was fit with both eq 2 and eq 3 (the two models). It was found that the data could be fit well to both models. In Tables II and III we give for each set of data the various parameters resulting from the least-squares fits.

As mentioned above, the compound $[Ni_2(trien)_2(C_2O_4)](ClO_4)_2$ was run at both low field (14.8 kG) and high field (54.3 kG). Fitting the low-field data to eq 2 gave $J = -17.3$ cm^{-1}, $g = 2.191$, and $\Theta = 4.7°$. The parameters resultant from the high-field data were essentially the same, only Θ is a little larger (5.6°). This increase in Θ cannot be attributed to magnetic field saturation (*i.e.*, $e^{-g\beta H/KT} \approx 1 + g\beta H/kT$) since saturation only affects the low-temperature region (<10°K), while Θ as well as the analogous $Z'J'$ (see Figure 1) is determined by the shape of the susceptibility curve in the vicinity of the peak, which is well above the saturation region. It is likely that the small difference between shapes of the low-field and high-field data which is responsible for the increase in Θ is merely a subtle experimental effect which is in any event within the limit of error that we have established. The low-field data for this same compound were also fitted to eq 3 and in this case we obtained $J = -15.7$ cm^{-1}, $g = 2.198$, $D = 13.7$ cm^{-1}, and $Z'J' = 0.28°$. It is clear that inclusion of zero-field splitting D does not appreciably alter the value of J (-17.3 *vs.* -15.7 cm^{-1}). Mention should be made of the uncertainty involved in the determination of D. It has been pointed out[5b] that the determination of D from magnetic susceptibility data cannot be done accurately. From an inspection of Figure 1 the difficulty is apparent. The size of D can be seen to be of appreciable importance only in the low-temperature and peak regions of the susceptibility curve. Near the peak, D is really of minor importance, so that even large values will not disturb the fit too much. In the lower temperature (<10°K) region, D is the only parameter that affects the susceptibility to any extent. This means that D will be the parameter that is forced to absorb various low-temperature phenomena not included in the susceptibility expressions used, such as magnetic-field saturation and the presence of small amounts of paramagnetic impurity. In the fitting to eq 3, we have kept D positive; however, a negative value of D could have been found that would have given as good a fit. Similar comments apply to the evalua-

tion of $Z'J'$ from a given data set. Thus only accurate values of J and g can be expected from fitting to eq 3.

Changing the tetramine ligand on the oxalate-bridged dimer does not change the J value appreciably. High-field data for $[Ni_2(macro)_2(C_2O_4)](ClO_4)_2$ fitted to eq 2 give $J = -18.4$ cm^{-1}. The small difference (0.8 cm^{-1}) between J values for the two different tetramine ligands on the oxalate dimer is probably well within experimental uncertainty limits.

Magnetic susceptibility data were collected for squarate-bridged $[Ni_2(macro)_2(C_4O_4)](ClO_4)_2$ at low field. Fitting to eq 2 gave $J = -1.3$ cm^{-1}, $g = 2.210$, and $\Theta = 1.6°$. The attenuation in magnetism (see Figure 4) in the squarate-bridged Ni(II) dimer is explained in this model by antiferromagnetic coupling to the extent of $J = -1.3$ cm^{-1}. This J is probably too large, because some of the attenuation in magnetism is most likely due to zero-field splitting. Thus, fitting to eq 3 gives $J = -0.42$ cm^{-1}, $g = 2.197$, $D = 15.5$ cm^{-1}, and $Z'J' = 0.48°$. Attempts to fit the squarate data to eq 3 with positive J failed.

In summary, theoretical fitting of magnetic susceptibility data has shown that the oxalate-bridged Ni(II) dimer is antiferromagnetic with $J \simeq -17$ cm^{-1}, whereas the interaction in the squarate-bridged dimer is on the order of $J \simeq -0.4$ cm^{-1}.

Exchange Mechanism. Recent reviews[2,19] dealing with the interpretation of exchange interactions have stressed the application of qualitative symmetry arguments to predict or explain the sign and magnitude of J, the exchange integral. It is recognized that when two metal ions are chemically bonded to a common set of closed-shell atoms, the unit comprising a bridged dimer system, any unpaired electrons originating from d orbitals on the metals will delocalize through extended molecular orbitals onto the bridge. The nature of the interaction between the unpaired electrons associated with the two metal centers is dictated by the relationship (*i.e.*, symmetry) between the atomic orbitals in which these electrons reside. If the unpaired electron from one metal has some probability of being in an orbital which has some p_y character on a given bridging atom and an extended orbital with an unpaired electron from the other metal ion overlap this same p_y orbital, then "kinetic exchange"[2] between these electrons will cause a splitting of spin states such that the lowest energy configuration of the electron spins is when they are aligned antiparallel. This results in antiferromagnetic interaction, which is thus just a weak bonding between the two metal ions propagated by the bridging ligand.

If the bridging situation is such that there is no direct overlapping of orbitals containing the two unpaired metal d electrons but instead the electrons are in molecular orbitals which are orthogonal to each other, then "potential exchange"[2] can take place, and the lowest energy configuration of the two spins will occur when they are parallel. As this state is increasingly populated at low temperatures, the magnetism of the dimer will increase rapidly, an effect referred to as ferromagnetic coupling. There is an increase in the potential energy of the dimer system by having the unpaired spins aligned in the ground state. This results from the spin polarization that occurs between the two unpaired electrons located in orthogonal orbitals.

The simplest example of a bridging system where these two mechanisms may be illustrated and the symmetry-
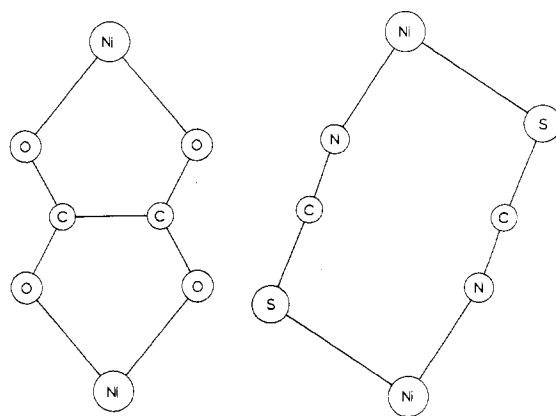

Figure 5. Structural features of the bis(thiocyanate)- and oxalate-bridged nickel(II) dimers. Both dimer units are approximately planar.

determined features pointed out is that where two metal atoms are bridged by a single atom, M–X–M. If the bridging atom is positioned directly between the two metal ions (MXM = 180°), then the metal d orbitals in which the unpaired electrons are located will overlap the same bridging atom orbital, say the p_y orbital. This will lead to a bonding situation and antiferromagnetic coupling. If MXM = 90°, then metal d orbitals containing the unpaired electrons would overlap with orthogonal bridging atom orbitals, say the p_y and p_x orbitals. There will be a mutual spin polarization between the two orthogonal systems, and the two unpaired electrons would couple ferromagnetically. In the transition to a polyatomic bridging situation, we are concerned with the symmetry of the various molecular orbitals and it must be noted that the exchange integral J is a sum of the contributions (in general both antiferromagnetic and ferromagnetic) from the various orbitals and unpaired electrons in the dimer unit.

The oxalate bridge can be viewed as a pseudo bis(triatomic) bridge. Magnetic susceptibility studies have appeared for only a few nickel(II) dimers. The only Ni(II) dimer studied with a triatomic bridge is $[Ni_2(en)_4(NCS)_2]I_2$.[2,5] This compound was found to be ferromagnetic and as such it is enlightening to compare molecular orbital symmetries, etc., with those for the antiferromagnetically coupled oxalate-bridged Ni(II) dimer studied in this work. Figure 5 depicts the geometries of the nickel thiocyanate and oxalate bridges. The X-ray crystal structure[20] of the thiocyanate-bridged dimer shows the dimer unit to be nearly planar (nickel and sulfur atoms are <0.1 Å off the plane described by carbons and nitrogens which are planar within experimental uncertainty). The structural features of the oxalate-bridged Ni(II) dimers have not been reported,[21] but in all other structures[7-11] with bridging oxalates, the oxalate moiety is found to be planar. The thiocyanate dimer may be classified approximately as having C_{2h} symmetry, while the oxalate dimer has D_{2h} symmetry. The difference in symmetries between these two systems will be shown to be the cause of the differing magnetisms.

Ginsberg[2,5] analyzed the ferromagnetism of the thiocyanate dimer in the following manner. The SCN⁻ bridge has for its highest filled molecular orbitals two σ orbitals and two π orbitals. It is easy to see from Figure 5 that ferromagnetic coupling will result in the case of this thiocyanate

(19) P. W. Anderson in "Magnetism," Vol. I, G. T. Rado and H. Suhl, Ed., Academic Press, New York, N. Y., 1963.

(20) A. E. Shvelashvili, M. A. Porai-Koshits, and A. S. Antsyshkina, *J. Strukt. Chem. (USSR)*, **10**, 552 (1969).

(21) An account of an unpublished structure is given in ref 13.

dimer. Considering one NCS⁻ bridge, the unpaired electrons on one nickel will bond to the nitrogen end of the thiocyanate with the σ orbitals of the bridge, while the unpaired electrons on the second nickel will bond through the π orbitals of the bridge. Thus the unpaired electrons from the two metal centers are delocalized into orthogonal bridge orbitals on each NCS⁻ bridge and a ferromagnetic effect is observed for this dimer.

Antiferromagnetic exchange of the oxalate-bridged Ni(II) dimer is also explicable on simple symmetry considerations. The oxalate bridge is *symmetric* in its interaction with the two nickel ions. If the unpaired electrons on one nickel ion are delocalized into a certain bridge molecular orbital, because of the symmetry of this bridge the unpaired electrons on the second nickel will also be delocalized into the same bridge molecular orbital. Thus, in the case of the oxalate-bridged nickel(II) dimer, there are only antiferromagnetic mechanisms operative. The e_g (O_h designation) orbitals on the nickel ions span the a_{1g} and b_{1g} representations in the D_{2h} point group. CNDO/2 calculations were completed on the oxalate dianion and it was found that in the ten highest energy filled orbitals there are two a_{1g} and two b_{1g} symmetry orbitals. Bonding propagated through these four bridge orbitals leads to the observed antiferromagnetic interaction.

The squarate-bridged system would, on the basis of the above discussion, be expected to display some antiferromagnetic coupling. The fact that the observed J ($\simeq-0.4$ cm^{-1}) is small can be qualitatively rationalized. In D_{4h} symmetry (appropriate for the squarate-bridged nickel dimer moiety), the unpaired d electrons would be in a_{1g} and b_{1g} symmetry orbitals. Comparison of CNDO/2 calculations on the oxalate and squarate dianions shows that in the case of squarate the appropriate symmetry bridge orbitals lie at lower energy than those in the oxalate dianion. Even further, the squarate dianion is larger than the oxalate dianion and this would result in smaller expectation values of $\hat{e}^2/r_{ij}$ for the various molecular orbitals.

Conclusion

Antiferromagnetic exchange has been detected in oxalate- and squarate-bridged nickel(II) dimers. It is shown that the symmetry of the bridge is crucial in determining the sign and magnitude of the exchange interaction between bridged metal atoms.

Cationic Acetylenic Platinum(II) Compounds and Their Derivatives. V. A Comparative Study with π-Olefinic Complexes

M. H. CHISHOLM and H. C. CLARK*

Cationic methylplatinum complexes *trans*-[PtCH₃(un){P(CH₃)₂C₆H₅}₂]PF₆, where un = an olefin, diene, allene, vinyl ether, allyl alcohol, and allylamine, have been prepared from the reaction of *trans*-[PtCH₃(acetone){P(CH₃)₂C₆H₅}₂]PF₆ with the appropriate unsaturated hydrocarbon un. With cyclopentadiene, [(h⁵-C₅H₅)Pt{P(CH₃)₂C₆H₅}₂]PF₆ and methane were formed, while for un = diallyl ether and allylacetamide a disproportionation reaction occurred leading to [PtCH₃-{P(CH₃)₂C₆H₅}₃]PF₆ and [PtCH₃(un)P(CH₃)₂C₆H₅]PF₆ in which un acts as a chelating ligand. π-Allene complexes were only stable below 0°; above this temperature insertion into the methylplatinum bond occurred with the formation of cationic π-allylic complexes. The nature of the platinum–olefin bond is discussed on the basis of vibrational and variable-temperature nmr spectra. The bonding, trans influences, and reactivities of these π-olefinic cations are compared to those observed in closely related (i) acetylenic complexes *trans*-[PtCH₃(RC≡CR'){P(CH₃)₂C₆H₅}₂]PF₆ and (ii) cationic hydride olefinic complexes *trans*-[PtH(un)(PR₃)₂]PF₆.

Introduction

Metal–olefin and –acetylene complexes both utilize a synergic bonding mechanism:[1,2] acetylene or olefin π to metal dsp and metal d to olefin or acetylene π^*. Therefore it is not surprising that analogous series of metal complexes are known, *e.g.*, {P(C₆H₅)₃}₂Pt(un) and [PtCl₃(un)]⁻ where un = an acetylene[3-9] or an olefin.[9-12] However, the formation of a stable metal–olefin complex does not necessarily imply the equally facile formation of a stable acetylene complex, and *vice versa*. While platinum complexes of the form [PtCl₃(un)]⁻ and PtCl₂(un)L, where L = pyridine or ammonia, are readily formed with simple olefins,[12,13] only acetylenes RC≡CR', with bulky or functional groups R and R', which can interact with the metal or one of the other

(1) M. J. S. Dewar, *Bull. Soc. Chim. Fr.*, 18, C79 (1951).

(2) J. Chatt and L. A. Duncanson, *J. Chem. Soc.*, 2939 (1953).

(3) E. O. Greaves and P. M. Maitlis, *J. Organometal. Chem.*, 6, 104 (1966).

(4) E. O. Greaves, C. J. L. Lock, and P. M. Maitlis, *Can. J. Chem.*, 46, 3879 (1968).

(5) J. Chatt, R. G. Guy, and (in part) L. A. Duncanson and D. T. Thompson, *J. Chem. Soc.*, 5170 (1963).

(6) J. Chatt, R. G. Guy, and (in part) L. A. Duncanson, *J. Chem. Soc.*, 827 (1961).

(7) G. R. Davies, W. Hewertson, R. H. B. Mais, P. G. Owston, and C. G. Patel, *J. Chem. Soc. A*, 1873 (1970).

(8) G. R. Davies, W. Hewertson, R. H. B. Mais, and P. G. Owston, *Chem. Commun.*, 423 (1967).

(9) F. R. Hartley, *Chem. Rev.*, 69, 799 (1969), and references therein.

(10) C. D. Cook and G. S. Jauhal, *J. Amer. Chem. Soc.*, 90, 1464 (1968).

(11) W. H. Badley, *Inorg. Chim. Acta Rev.*, 2, 7 (1968).

(12) M. Orchin and P. J. Schmidt, *Coord. Chem. Rev.*, 3, 345 (1968).

(13) W. C. Ziese, *Pogg. Ann.*, 21, 497 (1931).